J. Fluid Mech. (1986), *vol.* 170, *pp.* 461–477
Printed in Great Britain

On the formation of vortex streets behind stationary cylinders

By GEORGE S. TRIANTAFYLLOU, MICHAEL S. TRIANTAFYLLOU AND C. CHRYSSOSTOMIDIS

Department of Ocean Engineering, Massachusetts Institute of Technology, Cambridge, MA 02139, USA

(Received 10 June 1985 and in revised form 14 March 1986)

The formation of vortex streets behind stationary cylinders is found to be caused by an absolute instability in the wake immediately behind the cylinder. The inviscid Orr–Sommerfeld equation is used together with measured profiles at Reynolds numbers of (*a*) $Re = 56$ when the absolute instability provides a Strouhal number of 0.13; and (*b*) $Re = 140000$ providing a Strouhal number of 0.21, both in agreement with experimental values. At the subcritical $Re = 34$ the instability is of the convective type; i.e. the disturbance decays, being convected away once the external disturbance is removed, in agreement with experimental observations. Finally, the instability of the mode which causes a symmetric array of vortices is shown to be always of the convective type.

1. Introduction

Steady flow past a circular cylinder is characterized for a wide Reynolds-numbers range by the formation of a vortex street in the cylinder wake. Rayleigh (1945) first pointed out that formation of the vortex street is related to an instability of the cylinder wake. Later, Kovasznay (1949) attributed the vortex-street formation entirely to the wake instability, based on experimental observations. The mechanism by which the wake instability leads to a vortex-street formation has been illustrated by Abernathy & Kronauer (1962). They studied the instability of two infinite vortex sheets initially at a fixed distance apart using a numerical technique developed earlier by Rosenhead (1931). Their simulation demonstrated that the dynamic interaction between the two vortex sheets leads to the formation of two rows of 'clouds of vorticity', closely resembling the Kármán vortex street. The results obtained by Abernathy & Kronauer, however, do not indicate any preferred vortex spacing or frequency of formation like those reported in experiments. More detailed wake models than the one used by Abernathy & Kronauer are required to explain the preferred frequencies and vortex spacings commonly observed in wakes. For the case of a flat plate parallel to a uniform flow, stability calculations using measured velocity profiles of the wake far behind the plate have been performed by, among others, Sato & Kuriki (1961) (temporal instability) and Gaster (1965) (spatial instability). Detailed stability calculations using complex frequencies and wave-numbers have been performed by Mattingly & Criminale (1972) for the incompressible wake behind a thin airfoil, and by Koch (1985) for the compressible wake behind a blunt-edged plate.

For the case of the wake behind a stationary cylinder Fromm & Harlow (1963),

and then Jordan & Fromm (1972), predicted successfully the forces on a circular cylinder and the value of Strouhal number by employing the Navier–Stokes equations and a finite-difference scheme.

A number of investigators have used the inviscid flow equations by modelling the wake as two infinitely thin shear layers and introducing separation criteria for the boundary layer of the cylinder (Faltinsen & Petterson 1982; Sarpkaya 1979). The interaction between the boundary-layer flow and the wake field is of primary importance within this approach, which fails to predict a Strouhal number in the absence of additional, artificially imposed, criteria.

In the present paper the linear instability of the wake behind a stationary cylinder is analysed by considering the physically relevant singularities of the local dispersion relation of measured profiles behind the cylinder. This type of analysis can determine the nature of the wake instability, namely whether the wake instability is of the absolute, or of the convective type Bers (1983). If the instability is absolute, any initial disturbance grows at any fixed location and, after nonlinearities have limited the growth of the disturbance, a self-sustained oscillation of the wake is established. If, on the other hand, the instability is convective, any initial disturbance grows with time, but is concurrently convected away, eventually leaving the wake undisturbed. The main finding of the present paper is that formation of the vortex street is due to an absolute instability in the symmetric mode of the wake immediately behind the cylinder. The frequency of the absolute-instability mode agrees well with the experimentally measured frequencies of vortex streets. Such an approach is found to be effective for both low and high Reynolds numbers. Two sets of measured profiles are analysed. The first set, reported by Kovasznay (1949), are for $Re = 56$ and the mode of absolute instability provides a Strouhal number $St = 0.13$ in agreement with the value of 0.13 reported by Kovasznay (1949) and Roshko (1953). The second set, reported by Cantwell (1976), are for $Re = 140000$ and the mode of absolute instability provides $St = 0.21$, in good agreement with the average value of 0.20 reported by Roshko (1961).

It is also found that profiles measured at the subcritial number $Re = 34$ by Kovasznay (1949) provide a convective instability, in agreement with his observations of a disturbance decaying once the excitation is removed The antisymmetric instability is shown to be always of the convective type.

Finally, by studying a simple rectilinear profile it is shown that the instability of a profile with shear layers of small thickness is of the convective type, and hence is a poor model for the wake, while in the limit of zero thickness the problem becomes ill-posed.

2. Stability analysis

We shall consider the linear instability in the wake behind a stationary cylinder of diameter d. The linearized unsteady flow, modelled as inviscid and incompressible, forms on top of the laminar (or pseudo-laminar, for higher Reynolds-numbers) time-averaged flow field, which is assumed to be locally parallel. This last assumption is the most restrictive one, requiring in essence that at each section behind the cylinder the properties of the wake are adequately represented, locally, by the stability properties of a parallel flow having the same average velocity profile. The analysis of the wake, therefore, is decomposed into several equivalent parallel-flow problems, studied through the inviscid Orr–Sommerfeld equation, resulting in a 'strip-theory' approach.

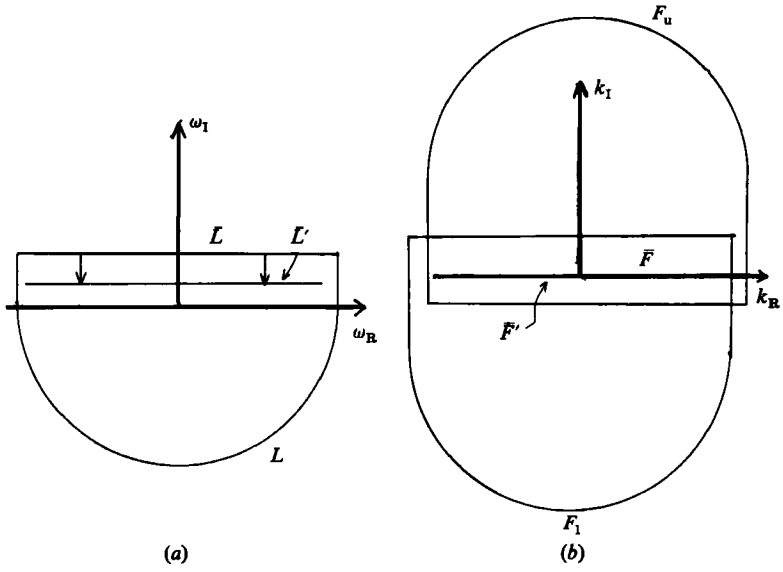

FIGURE 1. Integration countours in (*a*) the ω-plane; (*b*) the k-plane.

The effects of viscosity are neglected in the analysis of the parallel flows; the shape of the measured profiles, though, depends strongly on the Reynolds number, so viscosity indirectly plays a significant role. The results of the present analysis seem to justify this approach.

The linear stability properties of a parallel flow can be studied by considering the time and space evolution of a disturbance of finite spatial extent, which starts at time $t = 0$. The stream function representing a linearized disturbance is decomposed into an even and an odd part. The even part of the stream function ultimately causes a staggered array of vortices (Kármán street) and will be referred to as the *symmetric mode*, while the odd part, called here the *antisymmetric mode*, causes two symmetric rows of vortices. The stability of each mode is studied separately.

The criterion for distinguishing between absolute and convective instability in a homogeneous medium can be derived using a Laplace–Fourier transform method, best described by Bers (1983). Here only the main points of the method are outlined, and we refer to Bers for a complete discussion of the problem. The criterion can be obtained by studying the response $\psi(x, t)$ of the medium to an excitation that is localized in space and time. The response $\psi(x, t)$ can be obtained as an inverse Laplace–Fourier integral of the form

$$\psi(x,t) = \frac{1}{(2\pi)^2}\int_L \mathrm{d}\omega \int_F \mathrm{d}k \, \frac{1}{\Delta(\omega,k)}\, \mathrm{e}^{\mathrm{i}(kx-\omega t)}, \tag{1}$$

where $\Delta(\omega, k) = 0$ is the dispersion relation of the waveguide, ω is the frequency and k the wavenumber. Finally, L is a proper contour in the ω-plane and F the corresponding contour in the k-plane. Both ω and k are complex and we use the subscripts R to refer to their real part and I to their imaginary part.

Causality requires that all singularities must lie in the lower ω half-plane, below a line $\bar{L}$. In the k-plane we must perform two separate integrations, one for left-travelling waves ($x < 0$) and one for right-travelling waves ($x > 0$). The contour for the left-travelling waves we denote by F_l and that for the right-travelling waves by F_u. Since the disturbance is of finite spatial extent, it has a Fourier transform,

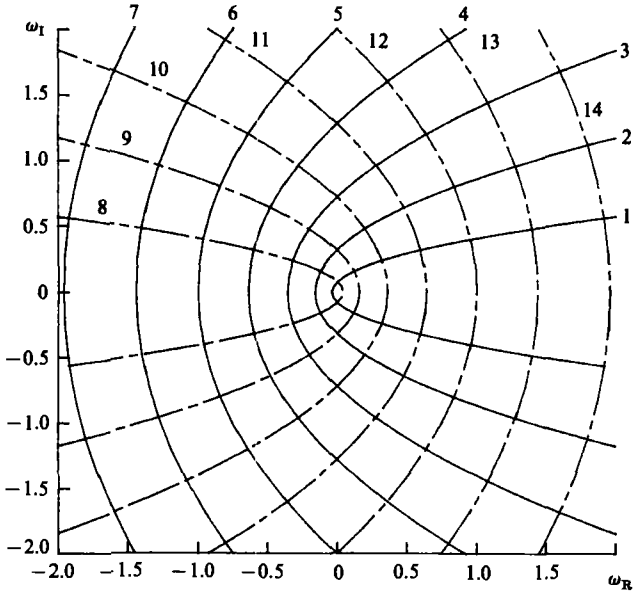

FIGURE 2. Plot of $\omega = k^2$ in the ω-plane for: ——, k_I = constant (curves 1–7, starting from 0.2 to 1.8 with increments of 0.2); — · —, k_R = constant (curves 8–14, starting from 0.2 to 1.8 with increments of 0.2).

so the real axis $\overline{F}$ must be within the region of convergence (ROC) of both left- and right-dwelling waves (figure 1).

$\Delta(\omega, k)$ plays an important role in determining the form of the instability: the map of $\overline{L}$ through $\Delta(\omega, k) = 0$ should have branches that do not cross $\overline{F}$, while the map of $\overline{F}$ in the ω-plane should lie entirely below the $\overline{L}$ line. Subject to these restrictions we lower the $\overline{L}$ line to $\overline{L}'$, while deforming $\overline{F}$ to $\overline{F}'$ appropriately, so as to place L' (if possible) on the ω_R axis, in which case a *convective instability* results.

If on the other hand the condition that the maps of $\overline{L}'$ on the upper and lower k half-plane do not cross $\overline{F}'$ is violated, we cannot lower the $\overline{L}'$ curve below the point where such a violation first occurs. The violation occurs when the two branches, F_u and F_l of the map of $\overline{L}'$ in the k-plane, touch at a point called the critical point (or 'pinch point' by Bers [1983]). If the map of the critical point in the ω-plane has a positive imaginary part, an absolute instability is obtained. If not, the instability is of the convective type.

The point where the upper and lower map of $\overline{L}'$ touch is a double root of the dispersion relation. Therefore, at this point the following relation is satisfied:

$$\frac{\mathrm{d}\omega(k_0)}{\mathrm{d}k} = 0. \tag{2}$$

For an analytic function $\omega(k)$ condition (2) implies that in the neighbourhood of $k = k_0$, ω behaves like a quadratic function of k,

$$\omega(k) - \omega(k_0) \sim \frac{\omega''(k_0)}{2!}(k - k_0)^2. \tag{3}$$

An orthogonal grid in the k-plane, therefore, is mapped on the ω-plane in the typical fashion of a quadratic function (figure 2 after Ahlfors [1966]). Such a criterion from the k- to the ω-plane is best suited to physical problems, where it is far easier to find ω as a function of k than the other way around, the reason being that $\Delta(\omega,$

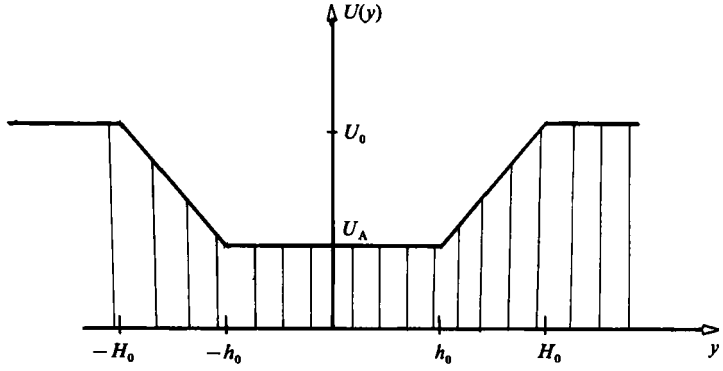

FIGURE 3. Simple wake profile used in figures 4–7.

k) is a polynomial function of ω resulting from Newton's law, while it is an arbitrary analytic function of k. This implies that for a given k, $\Delta(\omega, k) = 0$ can be solved in terms of a linear matrix eigenvalue problem, which is also employed here (see Appendix).

It should be noted that this method determines all double roots of the dispersion relation, irrespective of whether they are critical points. Therefore, after a double root of dispersion relation is determined, it should be verified that this double root results from the coalescing of two roots of the dispersion relation originating from opposite sides of the real k-axis.

3. Simple rectilinear wake model

We consider first the simple rectilinear wake velocity profile shown in figure 3. Such a rectilinear model contains the salient features of the wake required for stability calculations. This can be verified by comparing the results obtained in this section using the rectilinear wake model with results obtained in the following sections using measured wake velocity profiles.

The dispersion relation for the rectilinear velocity profile has been derived for k_R positive and is given by (symmetric mode)

$$\Delta(\omega, k) = A\omega^2 + B\omega + C = 0, \tag{4}$$

where

$$A = 2[1+\tanh(kh)], \tag{5}$$

$$B = -2\{[1+\tanh(kh)]\,ku_0+\Delta_0\} - [1+\tanh(kh)]\,(2k-\Delta_0) + \Delta_0 e^{-2k(1-h)}\{[1-\tanh(kh)]\}, \tag{6}$$

$$C = (2k-\Delta_0)\{[1+\tanh(kh)]\,ku_0+\Delta_0\} - \Delta_0 e^{-2k(1-h)}\{[1-\tanh(kh)]\,ku_0-\Delta_0\}. \tag{7}$$

The parameters h, Δ_0, k, ω and u_0 in (5)–(7) are defined as follows:

$$h = h_0/H_0, \tag{8}$$

$$\Delta_0 = (U_0-U_A)\,H_0/(\delta U_0), \tag{9}$$

$$\delta = H_0-h_0, \tag{10}$$

$$k = \tilde{k}H_0, \tag{11}$$

$$\omega = \tilde{\omega}H_0/U_0, \tag{12}$$

$$u_0 = U_A/U_0, \tag{13}$$

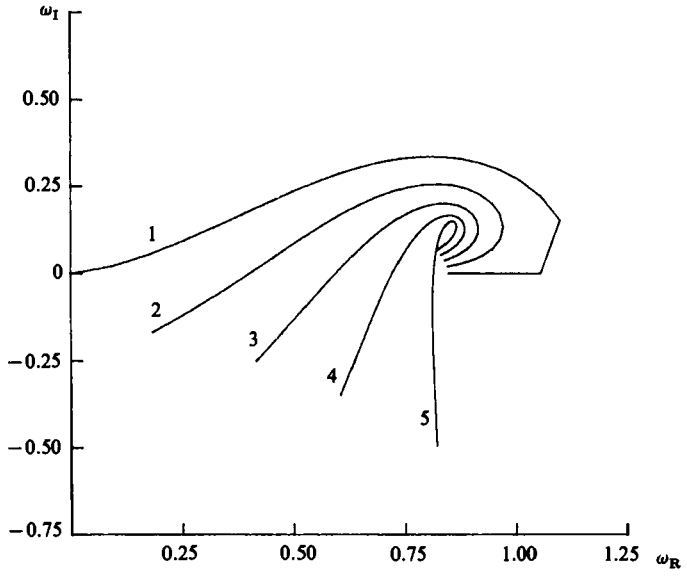

FIGURE 4. Map of lines k_I = constant in the plane for $U_A/U_0 = 0$, $h_0/H_0 = 0.3$. Curves 1–5 for $k_I = 0$ to -0.8 at increments of -0.20 (profile in figure 3).

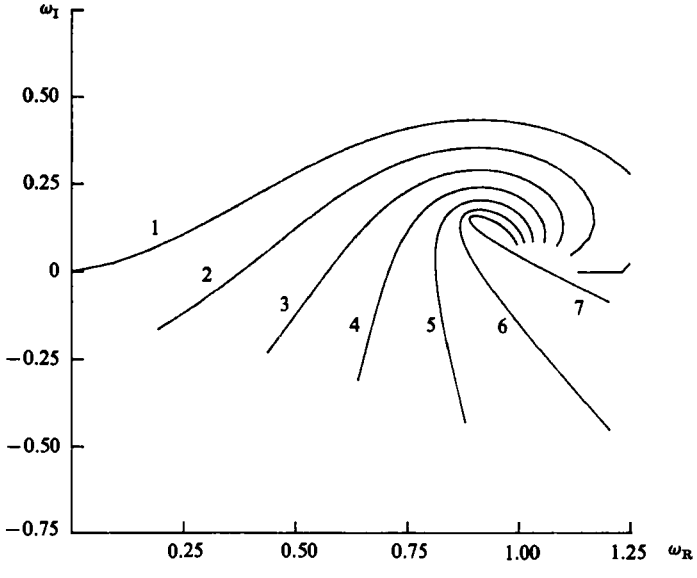

FIGURE 5. Map of lines k_I = constant in the ω-plane for $U_A/U_0 = 0$, $h_0/H_0 = 0.5$. Curves 1–7 for $k_I = 0$ to -1.2 at increments of -0.20 (profile in figure 3).

where δ is the thickness of the shear layer, H_0 is the half-width of the wake, U_0 the free-stream velocity, U_A the velocity at the centreline, $\tilde{k}$ the wavenumber and $\tilde{\omega}$ the wave frequency.

By mapping a rectangular grid in the k-plane to its image in the ω-plane via the $\Delta(\omega, k) = 0$ equation, the critical point can be identified by its local resemblance to the plot of a quadratic function. The ω_I *vs.* ω_R plots for constant k_I have a peak of

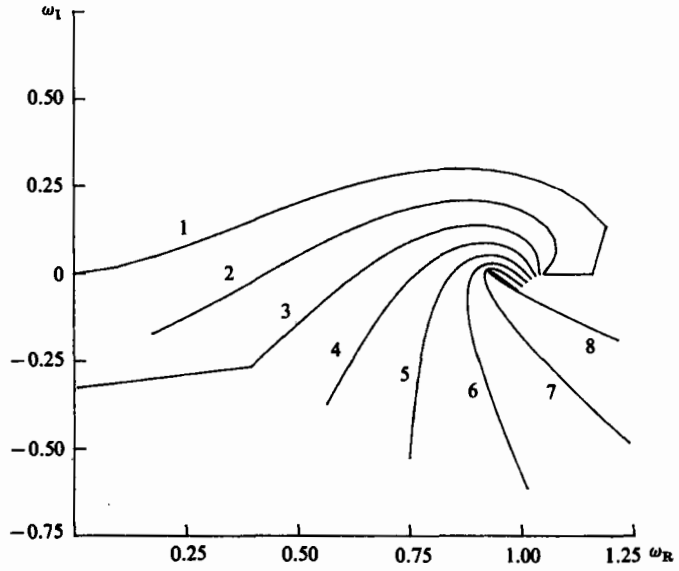

FIGURE 6. Map of lines k_I = constant in the ω-plane for $U_A/U_0 = 0.10$, $h_0/H_0 = 0.3$. Curves 1–8 for $k_I = 0$ to -1.4 at increments of -0.20 (profile in figure 3).

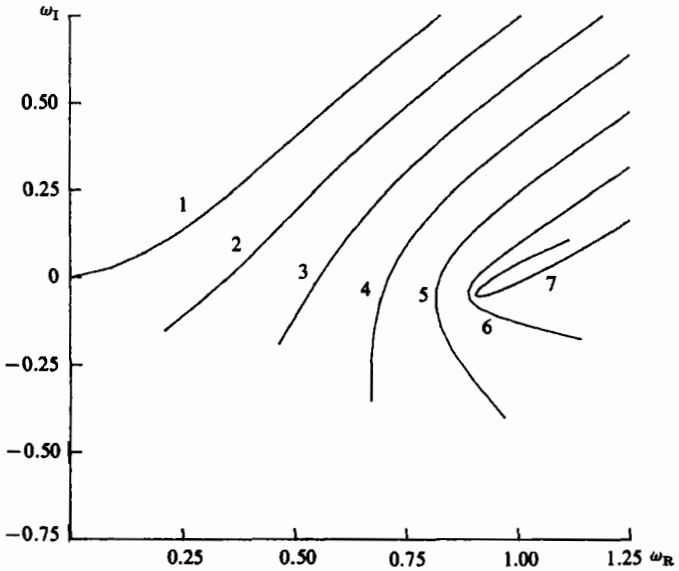

FIGURE 7. Map of lines k_I = constant in the ω-plane for $U_A/U_0 = 0$, $h_0/H_0 = 0.95$. Curves 1–7 for $k_I = 0$ to -1.2 at increments of -0.20 (profile in figure 3).

decreasing magnitude as k_I becomes more negative, until the double root of the dispersion relation is reached, when their shape changes substantially (figure 4).

After determining the double root of the dispersion relation, it was verified that this double root corresponds to the coalescence of two roots of the dispersion relation originating from opposite sides of the real-k axis.

If the critical point is positioned above the ω_R axis, we have an absolute instability, whereas if the critical point is positioned below the ω_R axis, we have a convective

x/d	A	a	b
2.0	0.53	2.25	0.52
3.5	0.56	1.60	0.50
5.0	0.58	1.00	0.25
8.0	0.36	0.55	0.25
20.0	0.20	0.20	0.25

TABLE 1. Curve-fitting parameters for Re = 56

instability. Since it is one of the principal points of this paper that vortex formation is due to an absolute instability near the cylinder, which turns into a convective instability further away from the cylinder, it is worth exploring the properties of this simple profile.

There are two basic parameters: $h = h_0/H_0$ and $u_0 = U_A/U_0$. Figures 4 and 5 show an absolute instability when $u_0 = 0$ and $h = 0.3$ (figure 4), or $h = 0.5$ (figure 5). For $u_0 = 0.1$ and $h = 0.3$ the critical point moves on the ω_R axis (figure 6) providing, marginally, a convective instability. Figure 7 is for $u_0 = 0$ and $h = 0.95$, corresponding to a profile closely resembling two thin shear layers. First we note that the critical point is below the ω_R axis, providing a convective instability. Also, the map of the k_R axis on the ω-plane has a maximum ω_I value which increases as h increases (figures 4 and 5), tending to infinity as h approaches 1. Within the present context, therefore, the problem of two infinitely thin shear layers is ill-posed since the $\overline{L}$ contour cannot be properly defined. These two observations should make methods employing infinitely thin shear layers suspect with respect to their ability to predict the frequency and wavenumber of instability waves.

This analysis provides the following basic conclusions: profiles with U_A/U_0 near zero, such as those close to the cylinder, support an absolute instability, provided that the thickness of the shear layers is not small. In fact, h_0/H_0 must lie in the range 0.2–0.8, with a maximum absolute instability at about $h_0/H_0 = 0.4$.

4. Vortex formation at low but above the critical Reynolds number

We first consider the formation of vortex streets in laminar wakes. Average wake velocity profiles were measured at various distances behind a cylinder by Kovasznay (1949). First we use his measured profiles for Reynolds number $Re = 56$, which is above the critical Reynolds-number limit for vortex-street formation of about 40.

The measured point data were fitted first by a curve

$$\frac{U(y)}{U_0} = 1 - A + A \tanh\left[a\left(\left(\frac{y}{d}\right)^2 - b\right)\right], \tag{14}$$

where A, a, b are curve-fitting parameters. The values of these parameters are given for $x/d = 2.0$, 3.5, 5.0, 8.0 and 20.0 in table 1. The fitting curve and the point data are shown in figures 8 and 9 for $x/d = 3.5$ and 8.0 respectively. Similar results are obtained for the other sections.

Stability analysis yielded the following result: for $x/d = 2.0$ there is an absolute instability at $\omega_R = 0.82$ with $k_R = 1.1$. The corresponding growth rates are $\omega_I = 0.037$ and $k_I = -1.1$. This is shown in figure 10 where the typical shape corresponding to $d\omega/dk = 0$ is seen at the right lower part of the graph.

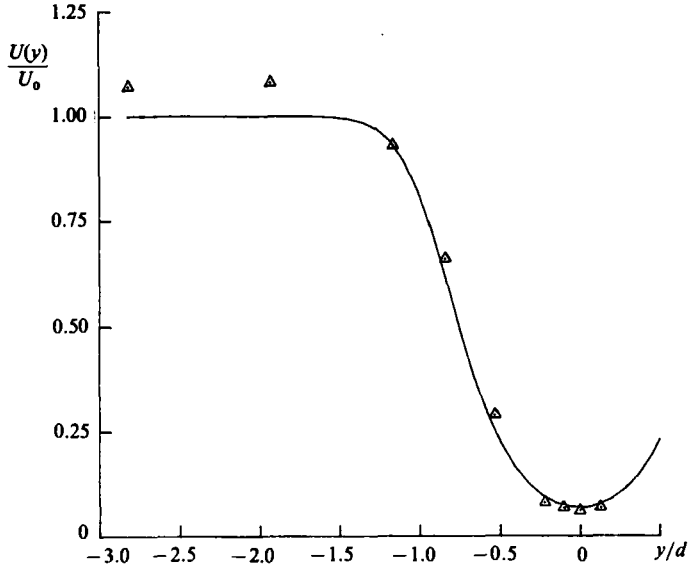

FIGURE 8. Average velocity profile at $x/d = 3.5$ for Reynolds number $Re = 56$: experimental data (△); fitted curve (——).

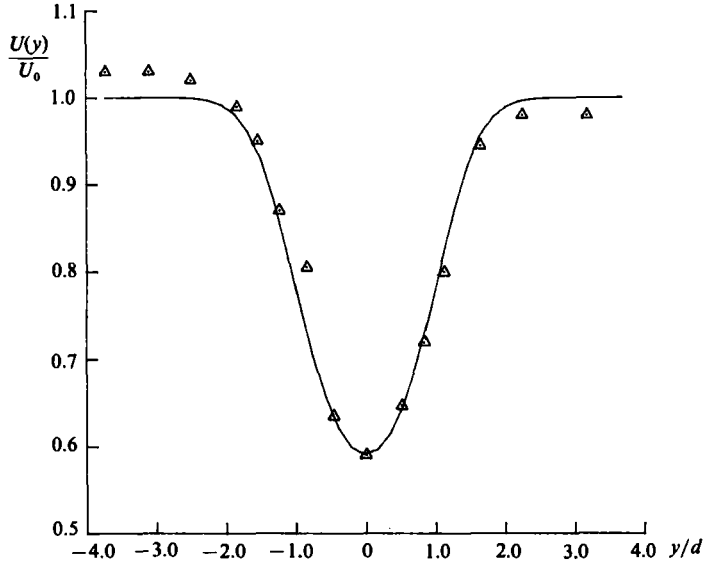

FIGURE 9. Average velocity profile at $x/d = 8.0$ for $Re = 56$: experimental data (△); fitted curve (——).

As we move away from the cylinder, the critical point moves gradually to lower values of ω_I, eventually crossing down the ω_R axis, providing a convective instability. Then the (ω_I, ω_R)-graphs are used to find the point of zero temporal growth. Figures 11–14 provide the stability results for $x/d = 3.5$, 5.0, 8.0 and 20.0 respectively. It is seen that the critical point moves on the ω_R axis for $x/d = 3.5$, while convective instability is obtained for the subsequent sections, whose spatial growth rate $-k_I$ is reduced the further we move away from the cylinder. This leads to the following

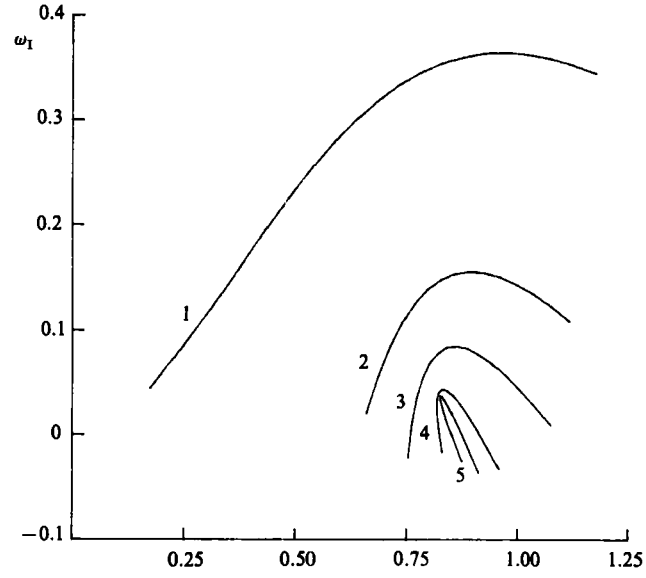

FIGURE 10. Map of lines k_I = constant in the ω-plane for the profile at $x/d = 2.0$ and Reynolds number $Re = 56$. $k_I + 0$ (curve 1); -0.50 (curve 2); -0.75 (curve 3); -1.0 (curve 4); -1.1 (curve 5).

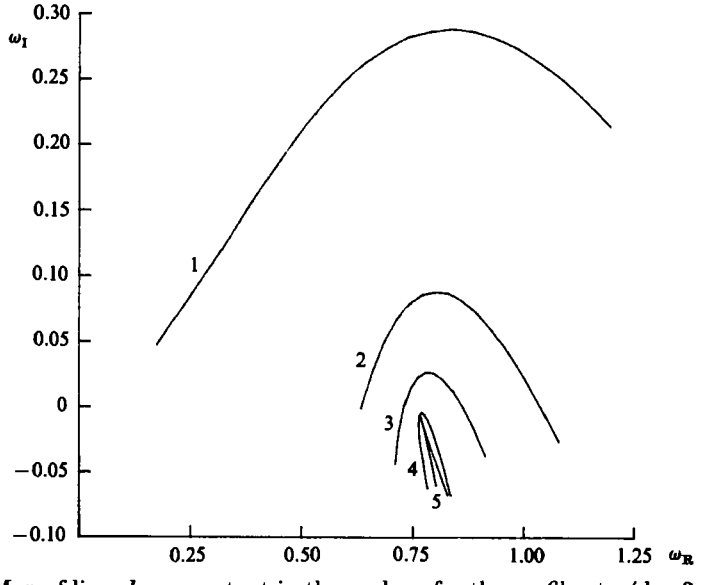

FIGURE 11. Map of lines k_I = constant in the ω-plane for the profile at $x/d = 3.5$ and $Re = 56$. $k_I = 0$ (curve 1); -0.50 (curve 2); -0.75 (curve 3); -1.0 (curve 4); -1.1 (curve 5).

instability scheme for vortex formation: immediately behind the cylinder the profile supports an absolute instability, causing perpetual motion once excited. As suggested by the results of the present analysis, it appears that the profiles supporting an absolute instability correspond loosely to the 'formation region' observed experimentally, which determines the real part of the frequency (Strouhal number) of the instability. The subsequent sections convect instability waves, driven continuously

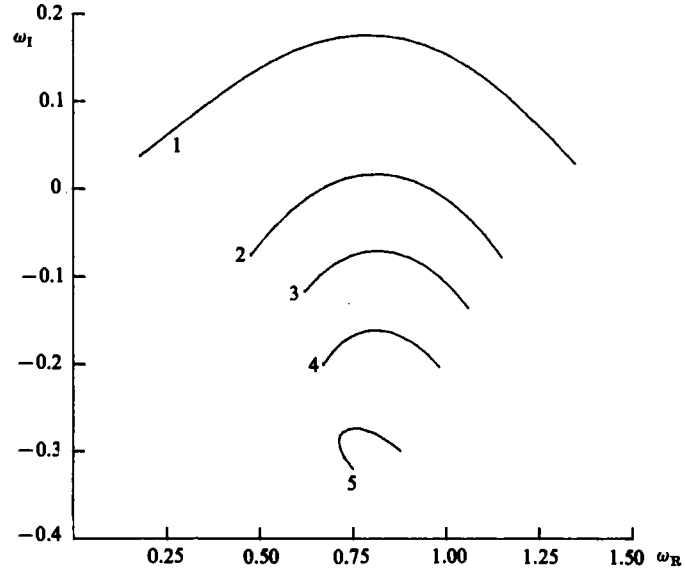

FIGURE 12. Map of lines k_I = constant in the ω-plane for the profile at $x/d = 5.0$ and $Re = 56$. $k_I = 0$ (curve 1); -0.30 (curve 2); -0.50 (curve 3); -0.75 (curve 4); -1.2 (curve 5).

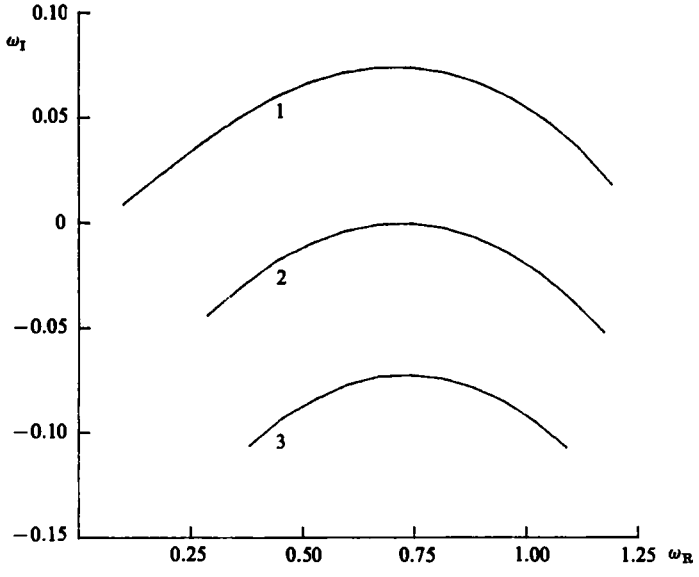

FIGURE 13. Map of the lines k_I = constant in the ω-plane for the profile at $x/d = 8.0$ and $Re = 56$. $k_I = 0$ (curve 1); -0.1 (curve 2); -0.2 (curve 3).

by the instability of sections behind the cylinder, so ω_R remains constant while k_R, k_I are modified as the dispersion relation requires.

Kovasznay (1949) reports a Strouhal number of 0.13 at $Re = 56$ and Roshko (1953) provides a similar value. As seen from figure 10, a value of $\omega_R = 0.82$ is obtained for the critical point, which corresponds to Strouhal number $St = \omega_R/2\pi = 0.13$, in agreement with experiment.

Table 2 provides the wavelength-to-diameter ratio and the spatial growth rate as

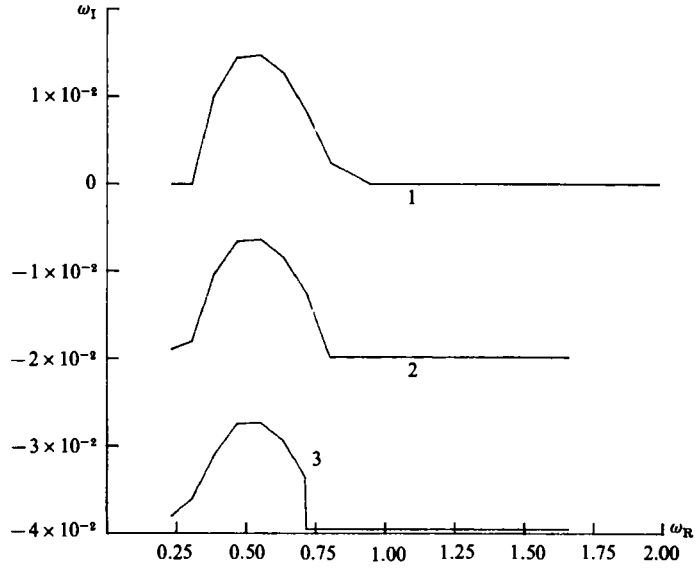

FIGURE 14. Map of lines k_I = constant in the ω-plane for the profile at $x/d = 20.0$ and $Re = 56$. $k_I = 0$ (curve 1); -0.025 (curve 2); -0.050 (curve 3).

x/d	ω_R	ω_I	k_R	k_I	λ/d
2.0	0.83	0.037	1.1	−1.15	5.46
3.5	0.83	0	1.45	−0.75	4.33
5.0	0.83	0	1.2	−0.30	5.24
8.0	0.83	0	1.05	−0.08	5.98
20.0	0.83	0	0.90	−0.01	6.98

TABLE 2. Frequency and wavenumber as a function of x/d for $Re = 56$

a function of the distance x/d behind the cylinder. It is seen that the growth rate diminishes away from the cylinder. We may note here the close qualitative similarity between the stability results of the simpler profiles analysed in the previous section and the results for the profiles measured by Kovasznay.

5. Vortex formation at below the critical Reynolds number

In the same paper Kovasznay (1949) measured velocity profiles for a Reynolds number of 34, a value below the critical Reynolds number for vortex-street formation of about 40. He reported that, at a Reynolds number of 34, the wake would form a vortex street only when externally excited, and that the vortex street would decay once the excitation was removed. An analysis of the profile at a distance of two parameters behind the cylinder was made using the following fitting parameters in (1):

$$A = 0.54, \quad a = 1.7, \quad b = 0.50.$$

The results of the stability calculations are shown in figure 15, where it can be seen that the wake is unstable, because the map of the real-k axis in the ω-plane lies above the real-ω axis, but the instability is convective because the critical point of the

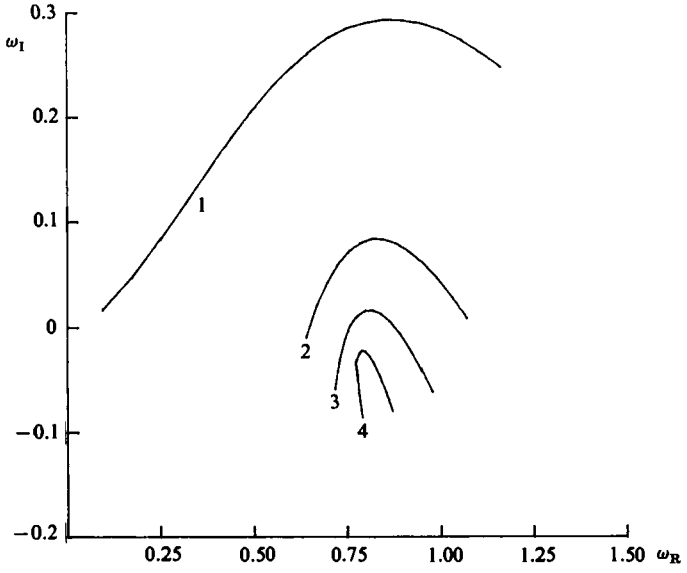

FIGURE 15. Map of lines k_I = constant in the ω-plane for the profile at $x/d = 2.0$ and $Re = 34$. $k_I = 0$ (curve 1); -0.50 (curve 2); -0.75 (curve 3); -1.00 (curve 4).

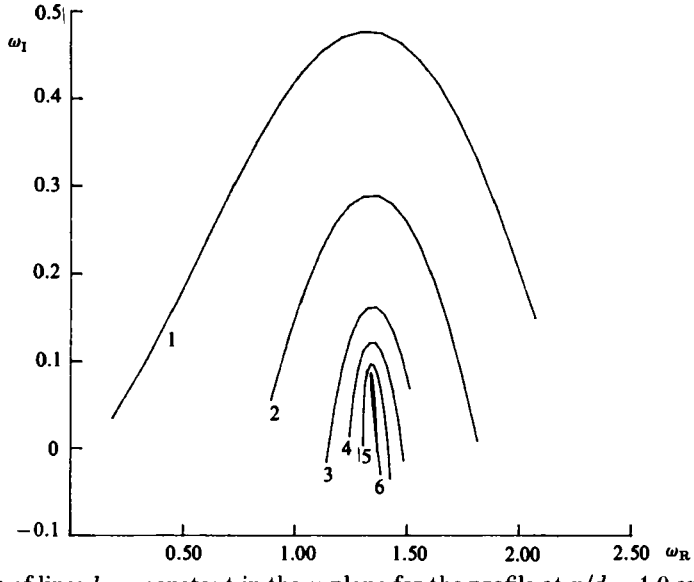

FIGURE 16. Map of lines k_I = constant in the ω-plane for the profile at $x/d = 1.0$ and $Re = 140000$. $k_I = 0$ (curve 1); -0.50 (curve 2); -1.00 (curve 3); -1.25 (curve 4); -1.50 (curve 5); -1.75 (curve 6).

dispersion relation lies below the real-ω axis. Due to the convective character of the instability, all disturbances will be convected away eventually leaving the flow undisturbed, in agreement with Kovasznay's observations. Thus, even though the wake is unstable, no vortex street is formed, a result that can be explained only through investigation of the character of the wake instability.

Comparing the results of this section with those of §4, we may conclude that when

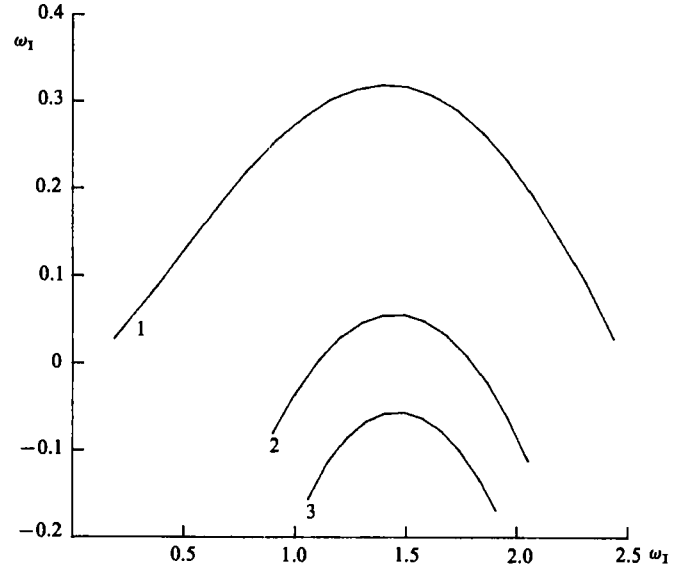

FIGURE 17. Map of lines k_I = constant in the ω-plane for the profile at $x/d = 2.0$ and $Re = 140000$. $k_I = 0$ (curve 1); -0.50 (curve 2); -0.75 (curve 3).

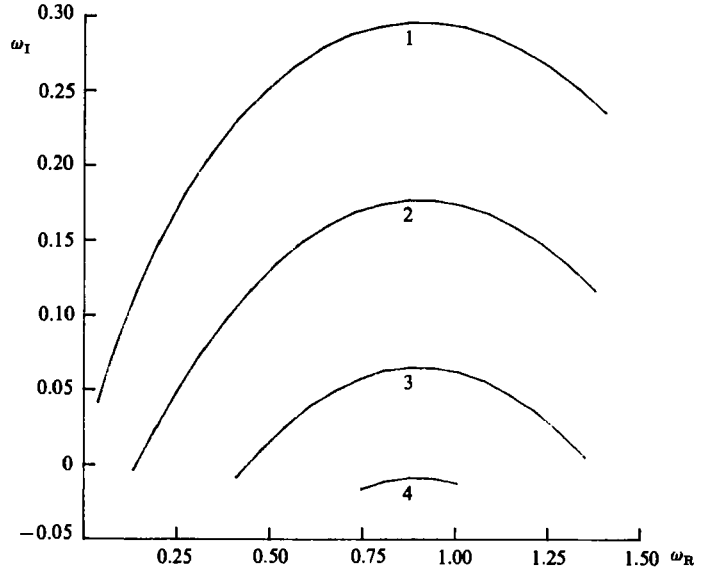

FIGURE 18. Map of lines k_I = constant in the ω-plane for the profile at $x/d = 2.0$ and $Re = 56$. $k_I = 0$ (curve 1); -0.20 (curve 2); -0.40 (curve 3); -0.54 (curve 4). Antisymmetric mode.

the Reynolds number reaches the value required for vortex-street formation, the critical point of the dispersion relation in the near wake first acquires a positive imaginary part. Thus, an absolute instability in the near wake is established leading to the formation of a vortex street, as previously discussed. The Reynolds number of the flow, therefore, strongly influences the vortex-street formation through the form of the average-velocity profile.

x/d	A	a	b
1.0	0.75	4.0	0.08
2.0	0.60	3.2	0.07

TABLE 3. Curve-fitting parameters for Profile at $Re = 140000$

6. Vortex formation at higher Reynolds numbers

We now consider the formation of vortex streets in turbulent wakes. A vortex street is known to exist in turbulent wakes, similar in form to that observed in laminar wakes, provided that the Reynolds number is below a critical limit of about 3×10^5. Stability calculations were performed using average-velocity profiles measured by Cantwell (1976) for a Reynolds number equal to 140000. The approach adopted here is similar to that outlined in Ho & Huerre (1984), namely it is considered that the instability waves form on top of a two-dimensional 'pseudo-laminar' flow, which is the time-averaged flow.

Stability calculations were performed at two stations in the wake using the parameter values given in table 3, the first located one diameter behind the cylinder, and the second two diameters behind the cylinder. The results are shown in figures 16 and 17 respectively. As can be seen in figure 16, at a distance $x/d = 1$ behind the cylinder an absolute instability exists, which is stronger than that of the laminar wake. At a distance $x/d = 2$ the instability is convective. Cantwell has estimated the formation region length to be about 2.2 diameters.

Cantwell (1976) reports a Strouhal number of 0.179 based on a free-stream velocity uncorrected for blockage effects, while Roshko (1961) summarizes results for Reynolds numbers near or above the transition Re, reporting a Strouhal number in the vicinity of 0.2 for $Re = 140000$. From figure 16 a value of $\omega_R = 1.3$ is obtained for the critical point, providing Strouhal number $St = 0.21$. The value of the temporal growth rate, ω_I is 0.087 and of the spatial growth rate k_I is -1.75. Finally, $k_R = 2.2$ providing that $\lambda/d = 2.85$. At $x/d = 2.0$ we obtain for the same frequency $k_R = 1.9$, which yields $\lambda/d = 3.3$. This is very close to the value of 3.24 reported in Tyler (1931).

The picture, therefore, as indicated by the results for both low and high (but below transition) Reynolds number is that of an absolute instability over a short distance immediately behind the cylinder, which corresponds to the 'formation region'. The length of the formation region is reduced as the Reynolds number is increased. The frequency of the vortex street is determined in the formation region. Also, the growth rate of the predominant instability wave increases with the Reynolds number, as can be verified by comparing the results for $Re = 56$ with those for $Re = 140000$.

7. Stability analysis of the antisymmetric mode

The antisymmetric part of the stream function is also unstable, yielding a symmetric arrangement of vortices, rather than the Kármán vortex street. If we consider the stability of the profile measured by Kovasznay at $x/d = 2.0$ at a Reynolds number of 56 (fitting parameters are given in table 1), we find that the instability is of the convective type, as shown in figure 18. It should be remembered that this profile has an absolute instability in its symmetric mode. The same result was found for the antisymmetric mode of the high-Reynolds-number flow. Therefore

it can be concluded that the symmetric part of a disturbance prevails both in laminar and turbulent wakes. As already mentioned, the symmetric-instability mode of the wake leads to an antisymmetric vorticity concentration. This implies that, both in turbulent and laminar wakes, the antisymmetric vorticity concentration will prevail, in agreement with the fact that the Kármán vortex street is always staggered.

8. Conclusions

Stability analysis of measured profiles immediately behind the cylinder showed an absolute instability, whose critical point predicts the Strouhal number of vortex-street formation: (*a*) at low but above the critical Reynolds number ($Re = 56$) the value of the Strouhal number is found to be $St = 0.13$ in agreement with the values reported by Kovasznay (1949) and Roshko (1953); (*b*) at high Reynolds number ($Re = 140000$) a value of $St = 0.21$ is found, in good agreement with the values reported by Roshko (1961).

Within the strip theory applied in this paper, the absolute instability of the near wake sets up a self-sustained motion, thus causing a continuous excitation for the rest of the wake. The frequency is set, therefore, by the absolute instability of the near wake, while the wavenumber varies along the length of the wake, as the local dispersion relation requires.

The analysis of the profiles at below the critical Reynolds number ($Re = 34$) showed that the instability is everywhere of the convective type, which agrees well with the observation by Kovasznay (1949) that a vortex street forms and lasts as long as an external excitation is applied.

The antisymmetric mode of the wake is found to be always of the convective type, so any arbitrary disturbance would invariably evolve into a symmetric one, in agreement with experimental observations.

The analysis of the simple rectilinear profile shows that a small centreline velocity and a finite shear-layer thickness provide an absolute instability. Layers of small thickness provide a convective instability, while in the limit the peak of the convective instability moves towards infinite k_R numbers and the problem becomes ill-posed within the present methodology, since no appropriate contour can be defined in the ω-plane. This agrees with the linear analysis of two shear layers as found, for example, in Abernathy & Kronauer (1962), which fails to provide a preferred mode, and the nonlinear simulation does not alter this result, as also shown in Abernathy & Kronauer.

The authors wish to thank Professor A. Bers of M.I.T. for providing many helpful suggestions and a preliminary version of Bers (1983).

Appendix. Solution of the inviscid Orr–Sommerfield equation

A matrix solution was obtained for the inviscid Orr–Sommerfield equation, expressed in terms of the stream function ψ

$$(kU-\omega)\left(\frac{\mathrm{d}^2\psi}{\mathrm{d}y^2}-k^2\psi\right)-k\frac{\mathrm{d}^2U}{\mathrm{d}y^2}\psi=0. \tag{A 1}$$

In (A 1) ψ is an even function of y for the symmetric mode (Kármán street) and an odd function for the antisymmetric mode (symmetric array of vortices) so the solution is reduced to $y \geqslant 0$, while the symmetry or antisymmetry about $y = 0$ is

used instead of a boundary condition. For y sufficiently large, the velocity profile is reduced to $U(y) = U_0$, and the curvature of the velocity profile becomes negligible. Consequently, the relation

$$\psi(y+\delta) = \mathrm{e}^{-k\delta}\psi(y) \quad (k_{\mathrm{R}} \geqslant 0, \quad y \gg d) \tag{A 2}$$

is applied to truncate the y-domain. A five-point centred finite-difference scheme was employed to reduce (A 1) together with (A 2) and the symmetry or antisymmetry condition into a generalized eigenvalue problem of the form

$$\omega \boldsymbol{B}(k)\,\boldsymbol{\psi} = \boldsymbol{A}(k)\,\boldsymbol{\psi} \tag{A 3}$$

where $\boldsymbol{A}, \boldsymbol{B}$ are $N \times N$ complex matrices, which are functions of k, and $\boldsymbol{\psi}$ is the complex eigenvector containing the values of the stream functions at the discretization points. The eigenvalue with maximum imaginary part is evaluated for any given k. A number of 50 discretization points was, typically, sufficient for accurate stability calculations.

REFERENCES

Abernathy, F. H. & Kronauer, R. E. 1962 The Formation of vortex streets. *J. Fluid Mech.* **13**, 1–20.

Ahlfors, L. V. 1966 *Complex Analysis*, 2nd edn. McGraw-Hill.

Bers, A. 1983 Basic Plasma Physics I. In *Handbook of Plasma Physics* (ed. M. N. Rosenbluth & R. Z. Sagdeev), vol. 1, chap. 3.2. North Holland.

Cantwell, B. J. 1976 'A flying hot wire study of the turbulent near wake of a circular cylinder at a Reynolds number of 140000'. Ph.D. thesis, California Institute of Technology, Pasadena, California.

Faltinsen, O. M. & Pettersen, B. 1982 Vortex shedding around two-dimensional bodies at high Reynolds number *Fourteenth Symp. on Naval Hydrodynamics, Ann Arbor, Michigan*, pp. 1171–1213.

Fromm, J. E. & Harlow, F. H. 1963 Numerical solution of the problem of vortex street development. *Phys. Fluids* **6**, 975–982.

Gaster, M. 1965 The role of spatially growing waves in the theory of hydrodynamic stability, *Prog. Aeron. Sci.* **6**, 251–270.

Ho, C. M. & Huerre, P. 1984 Perturbed free shear layers. *Ann. Rev. Fluid Mech.* **16**, 365–424.

Jordan, S. K. & Fromm, J. E. 1972 Oscillatory drag, lift and torque on a circular cylinder in a uniform flow. *Phys. Fluids* **15**, 371–376.

Koch, W. 1985 Local instability characteristics and frequency determination of self-excited wake flows. *J. Sound Vib.* **99**, 53–83.

Kovasznay, L. S. G. 1949 Hot-wire investigation of the wake behind cylinders at low Reynolds numbers. *Proc. R. Soc.* A, *Lond.* **198**, 174–190.

Mattingly, G. E. & Criminale, W. O. 1972 The stability of an incompressible two-dimensional wake. *J. Fluid Mech.* **51**, 233–272.

Rayleigh, Lord 1945 *Theory of Sound*, vol. II. Dover.

Rosenhead, L. 1931 The formation of vortices from a surface of discontinuity. *Proc. R. Soc. Lond.* A **134**, 170–192.

Roshko, A. 1953 On the development of turbulent wakes from vortex streets. *National advisory Comm. Aeronaut., Tech. Note* 2913.

Roshko, A. 1961 Experiments on the flow past a circular cylinder at very high Reynolds number. *J. Fluid Mech.* **10**, 345–356.

Sarpkaya, T. 1979 Vortex-induced oscillations. *Trans. ASME* E: *J. Appl. Mech.* **46**, 241–258.

Sato, H. & Kuriki, K. 1961 The mechanism of transition in the wake of a thin flat plate placed parallel to a uniform flow. *J. Fluid Mech.* **11**, 321–352.

Tyler, E. 1931 Vortex formation behind obstacles of various sections. *Phil. Mag.* **11**, 849–890.